ACS Pharmacology & Translational Science

pubs.acs.org/ptsci
Article

Systematic Quantitative Analysis of Fetal Dexamethasone Exposure and Fetal Lung Maturation in Pregnant Animals: Model Informed Dexamethasone Precision Dose Study

Ling Song,[#] Jie Song,[#] Ying Wang,[#] Yuan Wei,[*] Yangyu Zhao,[*] and Dongyang Liu[*]

Cite This: ACS Pharmacol. Transl. Sci. 2024, 7, 1770−1782

Read Online

ACCESS | Metrics & More | Article Recommendations | Supporting Information

ABSTRACT: Dexamethasone (DEX) was applied in neonatal respiratory distress syndrome treatment of pregnant women. We established a pharmacokinetics (PK)/pharmacodynamics(PD)/end point model of pregnant animals based on published data and then extrapolated to simulate fetal exposure and lung maturation in pregnant women. We first established the PK/PD/end point model for DEX in pregnant sheep. We considered the competitive effect of cortisol (Cort) and DEX binding with glucocorticoid receptor and then used the indirect response model to describe disaturated-phosphatidylcholine (DSPC) dynamics. Based on that, we established a regression relationship between DSPC and fetal lung volume (V40). We then extrapolated the PD/end point model of pregnant sheep to pregnant monkeys by corrected stages of morphologic lung maturation in two species. Finally, we utilized the interspecies extrapolation strategy to simulate fetal exposure (AUC_{0-48h}) and V40 relationship in pregnant women. The current model could well describe the maternal-fetal PK of DEX in pregnant animals. Simulated DEX AUC_{0-24h} values of the umbilical venous to maternal plasma ratio in pregnant sheep and monkeys were 0.31 and 0.27, respectively. The simulated Cort curve and V40 in pregnant sheep closely matched the observed data within a 2-fold range. For pregnant monkeys, model-simulated V40 were well fitted with external verification data, which showed good interspecies extrapolation performance. Finally, we simulated fetal exposure−response relationship in pregnant women, which indicated that the fetal AUC_{0-48h} of DEX should not be less than 300 and 100 ng/mL·hr at GW28 and GW34 to ensure fetal lung maturity. The current model preliminarily provided support for clinical DEX dose optimization.

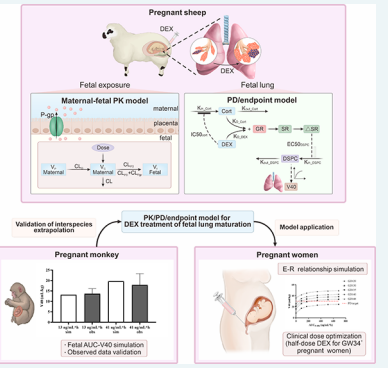

KEYWORDS: *DEX, pregnant women, PK/PD/end point model, fetal lung maturation*

Globally, approximately 15 million premature babies are born each year, constituting 35% of annual infant mortality cases.[1] Neonatal respiratory distress syndrome (NRDS) stands out as the most common complications associated with prematurity, causing significant morbidity in late preterm neonates and even leading to mortality in very low birth weight infants.[2] The incidence of NRDS is closely linked to gestational age at birth.[2] A multicenter study conducted in the United States between 2003 and 2007 revealed that 98% of babies born at 24 weeks experienced RDS, while at 34 weeks, the incidence dropped to 5%, and at 37 weeks, it was less than 1%.[3] In recent years, China has observed a growing trend in preterm birth rates with approximately 10% of all births occurring prematurely. NRDS also plays a substantial role in contributing to premature mortality in China, accounting for 12.9% of all newborn deaths.[4]

Currently, international guidelines recommend administering antenatal corticosteroids (ACS) therapy to pregnant women at risk of preterm birth between weeks 24 and 34 of gestation.[5] Dexamethasone (DEX) and betamethasone (Beta) are both synthetic glucocorticoids that easily cross the placenta and enter the fetal circulation, thereby promoting fetal lung maturation. They have been shown to significantly reduce the mortality rate of premature infants and the incidence of NRDS. Due to its lower cost and nearly identical biological activity compared to Beta, DEX has become the preferred choice for many developing countries, including China, in the management of threatened preterm labor.[5]

In 1969, Liggins demonstrated that DEX therapy markedly reduces the incidence and mortality of NRDS in preterm sheep.[6] Subsequently, they based on the dosages that employed in sheep experiments to recommend the clinical dosage regimen of DEX.[7] This dosage's effectiveness has been consistently validated over the past five decades, leading to its widespread adoption and use worldwide.[8] However, in the last two decades, more and more studies have indicated that the

Received: December 28, 2023
Revised: March 13, 2024
Accepted: March 15, 2024
Published: May 14, 2024

traditional DEX dosage regimen (5−6 mg Q12 h for 4 times) has yielded limited improvements. One study even demonstrated that clinical DEX treatment only reduced one-sixth risk of neonatal death and NRDS in preterm newborns.[9] Furthermore, numerous reports have raised concerns about the potential risk for long-term neurotoxic effects associated with the current classical dosage of DEX, particularly among pregnant women taking the medication during the third trimester or at full term.[10] Hence, there is an urgent imperative to optimize the clinical dosing regimen of DEX.

However, the dose−response relationship for DEX is currently unclear, which greatly impedes the efficient conduct of dose optimization research. On one hand, it is challenging to accurately describe the dose-fetal exposure relationship for DEX. Currently, most DEX pharmacokinetic (PK) studies primarily concentrate on simulating maternal blood levels.[11−13] Nevertheless, there remains substantial variability in predicting fetal blood drug concentrations.[14] On the other hand, establishing the fetal exposure-effect relationship for DEX is also challenging. The mechanism of DEX in promoting fetal lung maturation is complex, and it is difficult to directly obtain fetal lung maturity-related biomarkers (such as lung surfactant concentration like disaturated phosphatidylcholine (DSPC), surfactant protein A (SP-A, SP-B, SP-C, SP-D, etc.) and pharmacodynamics (PD) end points (such as lung ventilation, etc.).[15]

The model-informed study of pregnant animals' PK/PD/end point indicators is an effective approach for obtaining the quantitative relationship between fetal exposure and the therapeutic effects of DEX. The model-based meta-analysis approach has gradually gained popularity in recent years. This approach integrates information and knowledge from various sources and dimensions (different dosing regimens, different treatment durations, etc.). This approach fully utilizes literature data to establish mathematical models, addressing issues that cannot be resolved by single independent studies. Furthermore, it validates conclusions with external literature data, thereby increasing the strength of evidence.[16] The difficulty in establishing a fetal exposure-effect relationship is that fetal samples are not available clinically. At the level of pregnant sheep and pregnant monkeys, a large number of literatures have reported the mechanism of DEX promoting fetal lung maturation,[17,18] but no studies have established the fetal exposure-effect relationship based on these data. Jusko et al. established a quantitative relationship between intrauterine exposure and PD markers in pregnant mice, but the change of end point indicators were not considered in the pregnant mouse model.[19] At present, many literature studies have reported the end point indicators of lung maturation in pregnant sheep and pregnant monkeys, which can construct a complete quantitative relationship between fetal exposure, PD markers, and end point indicators, hoping to provide support for clinical dose adjustment.[20−23]

To sum up, this study hoped to establish a PK/PD model for DEX in pregnant sheep/monkeys based on a compartmental model. Ultimately, by simulating the dose-exposure-effect relationship of DEX in human fetuses using the pregnant sheep/monkey model throughout gestation, the study calculated the minimum effective dosage of DEX, hoping to provide a reference for dose adjustment when administering DEX to pregnant women for the prevention of NRDS.

1. RESULT

1.1. PK/PD Model Development in Pregnant Sheep.

The PK model parameters of pregnant sheep are shown in Table 1. The comparison of simulated and observed maternal and fetal DEX concentration−time curve in pregnant sheep at gestational days (GD)128 after single intramuscular injection was showed in Figure 1. The model could correctly fit the PK characteristics of DEX in both maternal and fetal sheep, but a 20% underestimation still existed at the maternal concentration maximum (C_{max}).

Table 1. Parameters of PK Model in Pregnant Sheep and Pregnant Monkeys

		pregnant sheep		pregnant monkeys	
parameters	description	value	CV (%)	value	CV (%)
Ka (h^{-1})[a]	absorption rate constant	25.1	3	0.33	7
CL/F (L/h)	clearance of central compartment	41	10	25.1	12
V_C/F (L)	volume of distribution in central compartment	1.01	13	3.97	12
V_P/F (L)	volume of distribution in peripheral compartment	119	14	35.9	7
CL_D/F (L/h)	distribution clearance between the central and peripheral compartment	276	8	23.5	8
CL_{PD} (L/h)	passive diffusion part of trans-placental clearance of DEX	23.9 FIX[b]		0.214	8
$CL_{p\text{-}gp}$ (L/h)	P-gp mediated active efflux part of trans-placental clearance of DEX	16.6	3	0.42	10
V_f/F (L)	volume of distribution in fetal compartment	0.492	20	3.26	1

[a]The administration route for sheep and money was intramuscular injection (i.m.) and oral administration. [b]Reference 24.

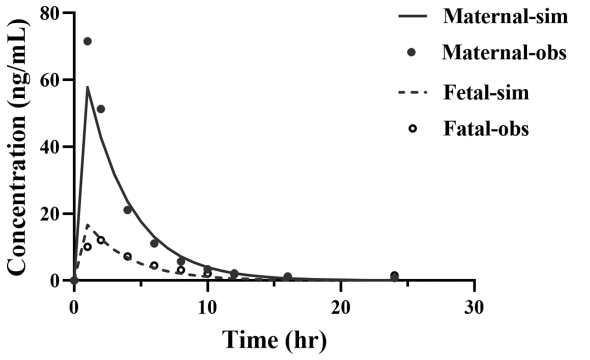

Figure 1. Observed and model-simulated maternal-fetal DEX concentration−time curve of pregnant sheep (GD128) within 24 h after a single intramuscular infusion of 12 mg sim is the predicted value, and obs is the observed value.

1.2. PD/End Point Model Development in Pregnant Sheep.

1.2.1. Cort/DEX and GR Binding Model. The physiological Cort concentration profiles ranged within GD110-GD145 and corresponding regression equations were shown in Figure 2A. Then, this regression curve was used as the baseline for subsequent modeling at different gestational stages. Figure 2B shows the Cort concentration curve under a single administration of DEX, which provided a good fit to the

https://doi.org/10.1021/acsptsci.3c00391
ACS Pharmacol. Transl. Sci. 2024, 7, 1770−1782

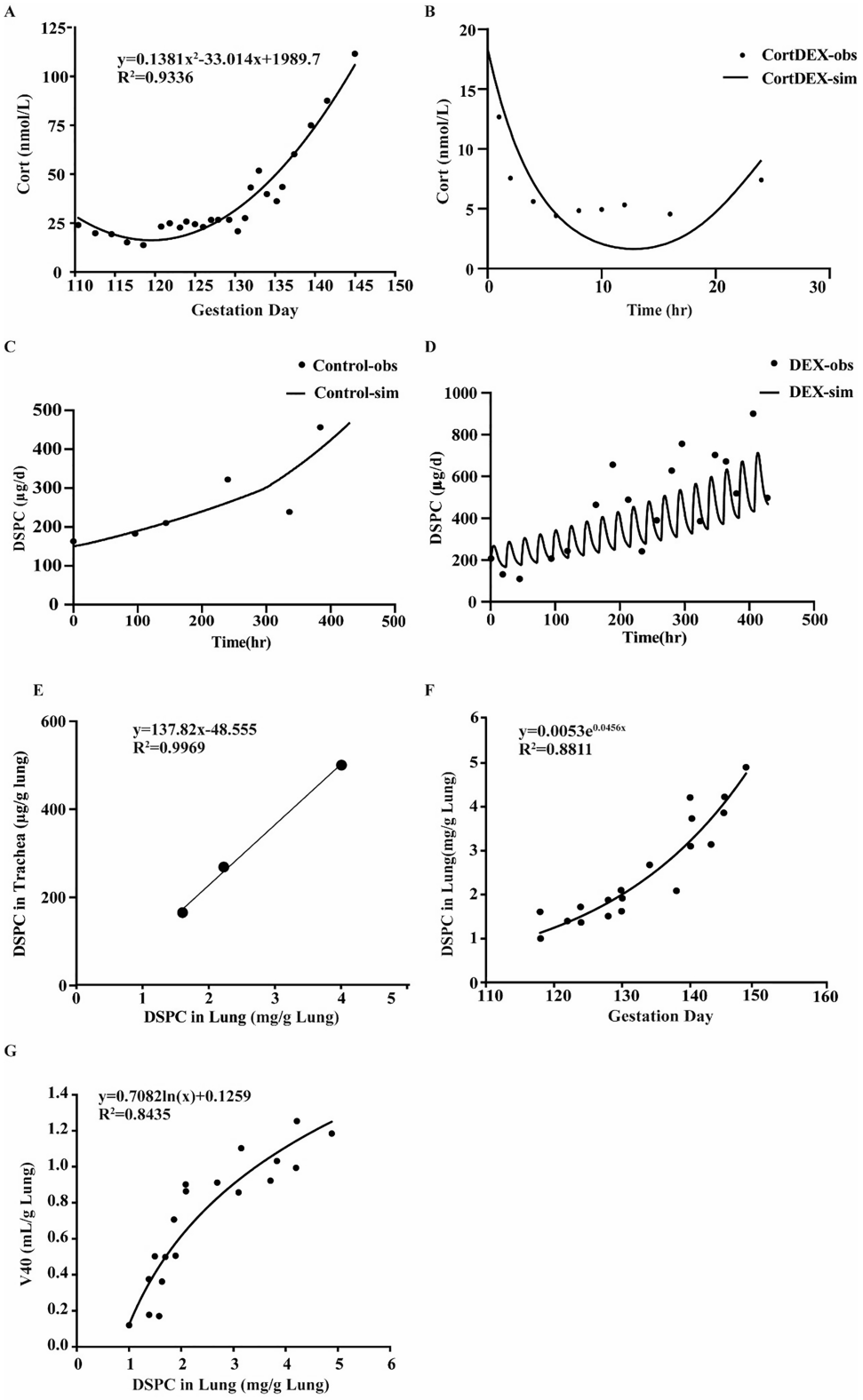

Figure 2. PD-end point model in pregnant sheep. (A) Developmental dynamics curve of Cort concentration with gestational age in fetal sheep; (B) Cort curve of pregnant sheep (GD123) after single intramuscular injection of DEX; (C, D) DSPC curve of fetal sheep (GD123) after daily injection of negative control (C) and 400 μg DEX (D). (E) Linear regression of DSPC_tracheal and DSPC_lung in fetal sheep; (F) dynamic curves of fetal sheep DSPC lung concentration with gestational age; (G) linear regression of DSPC lung concentration and V40 in fetal sheep.

observed Cort data. The Cort concentration was slightly underestimated during 6−17 h after dosage, which was also within a 2-fold error range. The sensitive analysis results revealed that the current underestimation of the Cort level had a minimal effect on fetal V40 estimation, as illustrated in Figure S1. Specially, when the Cort level decreased 10-fold, fetal V40 decreased marginally from 39.9 to 38.7 mL/g lung. In addition, after DEX administration, the Cort concentration was

https://doi.org/10.1021/acsptsci.3c00391
ACS Pharmacol. Transl. Sci. 2024, 7, 1770−1782

extremely inhibited around 5 ng/mL, which was difficult to play its role in promoting fetal lung maturation due to its lower affinity compared with DEX.[25] Both DEX and Cort bonded to the GR with different affinity constants (K_{D_Cort} and K_{D_DEX}).

1.2.2. SR Complex-DSPC Model. The predicted and observed profiles of DSPC amount in the daily tracheal secretion fluid (DSPC_trachea) in control and DEX treatment groups are shown in Figure 2C,D. Despite the considerable variability of DSPC_trachea, the model could effectively capture the growth trend of DSPC, especially for the low to middle range of observation. In the current model, focusing on the fitting for the low to middle range of DSPC provided more valuable information for recommending the minimum clinical effective dose. This is because the DSPC-driven fetal lung maturation follows a saturation process, as supported by recent research indicating that high DSPC concentration leads to a saturated fetal lung maturation effect.[26] This conclusion was further corroborated by our own results, as showed in Figure 2G, where DSPC concentration exceeding 600 ng/mL demonstrates a saturation trend of their promotion effect on fetal lung maturation.

1.2.3. DSPC-Disease End point (V40) Model. We used the DSPC_trachea data to develop the current DSPC model, since most of the published DSPC data were collected from tracheal secretions samples. However, this data could not directly represent the DSPC secretion amount per gram fetal lung tissue (DSPC_lung), which limited the link to end point of fetal lung volume of fetal sheep under trachea pressure of 40 cm H_2O (V40). We developed a linear regression to describe the relationship between mean values of DSPC_trachea[23] and DSPC_lung[27] during GD120−148 of pregnant sheep based on published data, as shown in Figure 2E.

We applied the regression equation to translate the DSPC_trachea to DSPC_lung at the individual level. The range of individual DSPC_ trachea was within 100−500 μg/d and the range of individual DSPC_lung within 1−4 mL/kg. Then, we conducted regression analysis between model simulated DSPC_lung and gestational age, as shown in Figure 2F.

Finally, we developed the regression analysis of individual DSPC_lung and V40 data, as shown in Figure 2G, which represented a significant correlation between DSPC and V40. All the PD-end point model parameters are shown in Table 2.

1.3. PK/PD Model Verification in Pregnant Sheep. The model simulated V40 was closed to the median values that published in two external verification literature studies of pregnant sheep, as shown in Figure 3A,B. There is a slight overestimation in the prediction for published fetal V40,[28] with errors within a 2-fold range. The model simulated and observed PK/PD parameters are shown in Table 3.

1.4. PK/PD Model Development and Verification in Pregnant Monkeys. The simulated and observed PK profiles in nonpregnant monkeys are shown in Figure 4A. The simulated and observed maternal and fetal PK profiles in pregnant monkey are shown in Figure 4B. The PK model parameters of pregnant monkeys are shown in Table 1. The model showed that the UV:MP ratio of AUC_{0-24} of DEX fetus was 0.27, which was similar to that of pregnant sheep (simulated UV:MP ratio of 0.31 and observed UV:MP ratio of 0.27) (shown in Table 3). Then, we simulated the fetal exposure of monkey based on the study design of literature that only published the V40 in fetal monkeys, as shown in Figure 4C. Subsequently, the V40 level was simulated at DEX dosage levels of 0.04 and 0.15 mg/kg with the corresponding fetal AUC_{0-24h} values of 13 and 41 ng/mL·h, as shown in Figure 4D. The model simulated V40 could well fitted the observed data, which verified the current PD/end point model extrapolation between various species. The model simulated and observed PK/PD parameters are shown in Table 3.

Table 2. Parameters of PD Model in Pregnant Sheep

parameters	description	value	CV(%)	source
GR (fmol/mg protein)	Glucocorticoid receptors	627 FIX		ref 28
$Cort_{bl}$ (nmol/L)	Baseline level of Cort	18.29 FIX		ref 28
K_{D_Cort} (nM)	Dissociation constant between Cort and GR	1280	0 FIX	model fitted
K_{D_DEX} (nM)	Dissociation constant between DEX and GR	3.29 FIX		ref 28
$IC50_{Cort}$(nM)	Half-maximum inhibitory concentration	0.0573	91	model fitted
K_{out_Cort} (h^{-1})	Elimination rate constant of Cort	0.237	31	model fitted
$DSPC_{bl}$ (μg/d)	Baseline level of DSPC of tracheal outflow	125.25 FIX		ref 23
$EC50_{DSPC}$ (fmol/mg protein)	Half-maximum effective concentration of DSPC	3.32	0 FIX	model fitted
$Emax_{DSPC}$ (μg/d)	Maximum effective effect of DSPC	219	0 FIX	Model fitted
$Kout_{DSPC}$ (h^{-1})	Elimination rate constant of DSPC	0.164	0 FIX	Model fitted

1.5. PK/PD/end point Model Simulation and Extrapolation of Effective Human Exposure. We simulated the exposure (AUC_{0-48h} of DEX)-response (V40) relationship in pregnant sheep at GD120, 130, 135, 140, and 148, as shown in Figure 5. We selected the AUC_{0-48} as the exposure metric based on the DEX clinical dose regimen (Q12h for 4 times). Based on the morphologic lung maturation stages of sheep and human,[25] it showed that the morphologic lung maturation stages of GD120, 140, and 148 in fetal sheep was similar to those of 28, 36, and 40 gestational weeks (GW) in human fetus, respectively.[30] The effective exposure was defined as the AUC_{0-48h} that reached the targeted end point as V40 equals to 30 mL/kg.[31] The effective AUC_{0-48h} of DEX at GD120 and GD135 in pregnant sheep was 300 and 100 ng/mL·h. We assumed that the effective exposure was consistent in fetal sheep and human fetus. Hence, in order to get an effective promotion to fetal lung maturity, the clinical DEX exposure of AUC_{0-48h} should not be less than 300 and 100 ng/mL·h at GW 28 and GW 34. The current effective exposure of DEX in human fetus provided a good indicator for clinical DEX therapeutic dose.

2. DISCUSSION

In this study, we established a quantitative PK/PD/end point relationship by fully considering the mechanism that DEX promotes fetal lung maturation: (i) For the PK part, a maternal-fetal DEX PK model was established to qualify the fetal exposure by involved the P-gp mediated trans-placental process of DEX. (ii) The DEX/Cort-GR relationship was developed by considering the competitive effect of DEX and Cort binding to GR as well as the DEX inhibition effect of Cort. (iii) The SR complex was used to drive the efficacy marker DSPC using an IDR model. The DSPC and disease end point indicator V40 were linked according to the regression relationship. Sensitivity analysis was performed to

https://doi.org/10.1021/acsptsci.3c00391
ACS Pharmacol. Transl. Sci. 2024, 7, 1770−1782

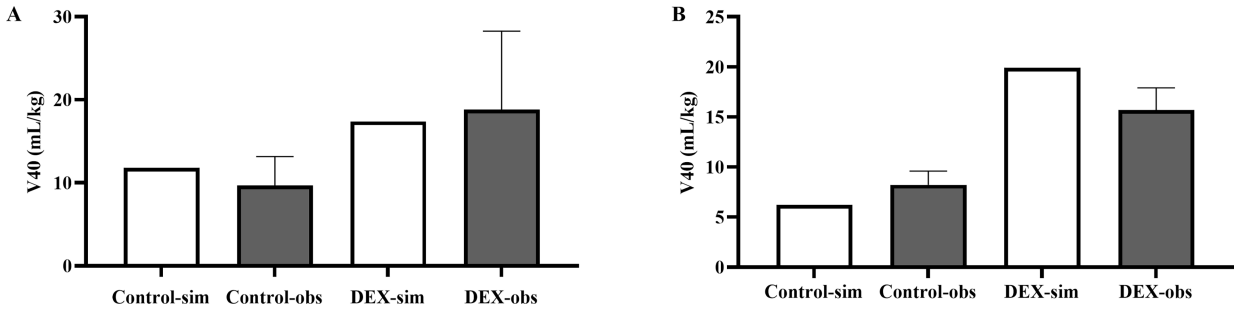

Figure 3. PD-end point model verification in pregnant sheep and monkeys. (A, B) Simulated and observed V40 results of fetal sheep with DEX intramuscular injection or not (control) of different literature studies.[20,29] The white column is the simulated result, and the gray column is the observed value; data are presented as mean ± SD.

Table 3. Observed and Simulated PK/PD Parameters of DEX in Pregnant Animals

model	species	dosage regimen[a]	parameters[b]	unit	sim[c]	obs[d]	ratio[e]
PK	pregnant sheep	12 mg single dose (i.m.)	Cmax-m	ng/mL	57.7	71.5	0.81
			CL-m	L/h	53.9	48.4	1.11
			AUC $_{0-24}$-m	ng/mL·hr	223	241	0.93
			Cmax-f	ng/mL	12.1	16.6	0.73
			AUC $_{0-24}$-f	ng/mL·hr	69.3	64.2	1.08
			UV:MP	NA	0.31	0.27	1.17
	pregnant monkeys	0.15 mg/kg single dose (oral)	Cmax-m	ng/mL	19.9	NA	NA
			CL-m	L/h	0.9	NA	NA
			AUC $_{0-24}$-m	ng/mL·hr	165	NA	NA
			Cmax-f	ng/mL	3.4	NA	NA
			AUC $_{0-24}$-f	ng/mL·hr	44.8	NA	NA
			UV:MP	NA	0.27	NA	NA
PD	pregnant sheep[f] (verification)	6 mg Q 12 h for 4 times (i.m.)	V40	mL/g lung	17.4	18.8 (9.39−28.3)	0.93
		0.25 mg/kg Q 24 h for 2 times (i.m.)			19.9	15.7 (13.5−17.9)	1.27
	pregnant monkeys (verification)	0.04 mg/kg Q 6 h for 4 times (oral)	V40	mL/g lung	13.2	13.7 (11.3−16.1)	0.96
		0.15 mg/kg Q 12 h for 3 times (oral)			19.7	17.9 (12.5−23.3)	1.10

[a]The administration route for sheep and money was intramuscular injection (i.m.) and oral administration. [b]Cmax: maximum concentration within 24 h; CL: clearance; AUC $_{0-24}$: area under curve within 24 h; UV/MP: the ratio of AUC $_{0-24}$ ratio of umbilical venous to maternal plasma. [c]Sim: physiologically based pharmacokinetic model simulated results. [d]Obs: clinical observed data. [e]Ratio: the ratio of mean value of sim/obs. [f]The observed V40 data of pregnant sheep was represented the median (range).

assess the sensitivity of input parameters concerning the estimation of fetal V40, as graphically shown in Figure S2. Core PK parameters (CL, $CL_{p\text{-}gp}$, V_f) and all PD parameters exhibited moderate or high sensitivity levels for fetal V40 estimation, which suggested that the current model encapsulates the key processes related with the effect of DEX on fetal lung maturation. Based on this model structure, we developed a comprehensive PK/PD/end point model in pregnant sheep. Subsequently, we used the same model structure to qualify the PD/end point relationship in pregnant monkeys after correction of the stages of morphologic lung maturation in different species. Thereby, current model provided good interspecific extrapolation performance for DEX-induced fetal lung maturation. Finally, we applied the PK/PD/end point model of pregnant sheep to pregnant women by correcting the gestational stages of morphologic lung maturation between different species. This study preliminarily provided an approach to achieved the clinical effective exposure DEX in different gestational phase.

This study simulated the clinical fetal effective exposure of DEX to promote lung maturation at various gestational stages. Current results indicated that the earlier the gestational week, the higher the exposure level of DEX required for fetal lung maturation. The effective DEX exposure of 34 GW was only one-third of that in 28 GW. In our another maternal-fetal PK study of DEX in pregnant women, the clinical fetal AUC_{0-48h} of DEX in late trimester was around 200 ng/mL·h under current clinical dose regimen of 5 mg DEX Q12h for 4 times (unpublished data). This exposure was 2-fold of effective exposure 100 ng/mL·h for lung maturity end point of V40 around GW34 (equals to 135 GD in pregnant sheep as shown in Figure 5). Our clinical maternal-fetal PBPK model of DEX also simulated the exposure of half-dose of DEX (2.5 mg Q12h 4 times) in the late trimester, resulting in an exposure of 97 ng/mL h (unpublished data). The above results indicated that a half-dose of DEX could effectively promote human fetal lung maturity. This finding is consistent with the results of betamethasone (Beta) clinical trials for women at risk of preterm delivery given half-dose versus full dose.[32] This study showed that the neonatal outcomes related to fetal lung maturity in the half-dose group was similar to that of standard-dose after 34 GW. However, around 28 GW, infants exposed to half-dose Beta had an increased risk of developing NRDS and requiring exogenous surfactant therapy.[32] Based on the above proof, we are undergoing another clinical trial involving the administration of half-dose DEX (2.5 mg Q12h for 4 times) to pregnant women after 34 GW, which aims to offer an

https://doi.org/10.1021/acsptsci.3c00391
ACS Pharmacol. Transl. Sci. 2024, 7, 1770−1782

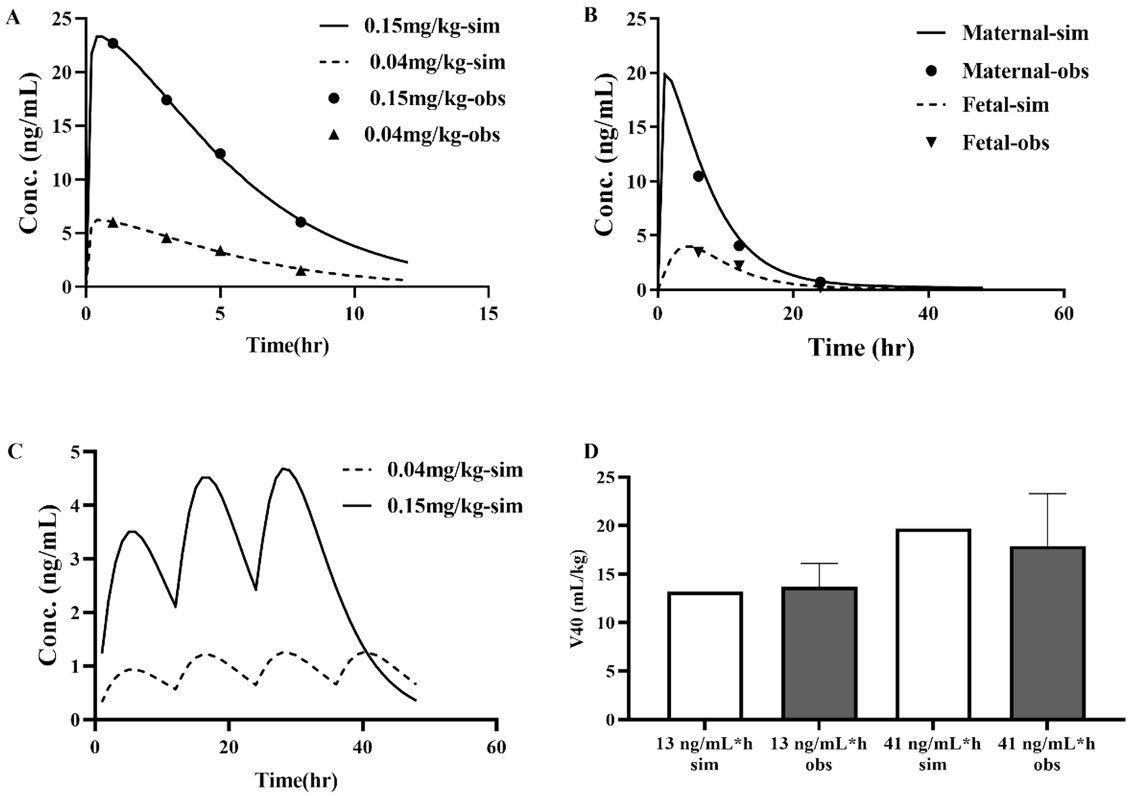

Figure 4. PK/PD model development and verification in pregnant monkeys. A, Simulated and observed DEX concentration−time profiles in nonpregnant monkeys; B, Simulated and observed maternal-fetal DEX concentration−time profiles in pregnant monkeys; C, prediction of DEX concentration−time curves in fetal monkeys at 0.04 and 0.15 mg/kg doses; D, simulated and observed V40 in fetal monkeys at doses of 0.04 and 0.15 mg/kg(corresponding fetal AUC_{0-24h} of 13 and 41 ng/mL·h), the white column is the simulated result, and the gray column is the observed value, Data are presented as mean ± SD.

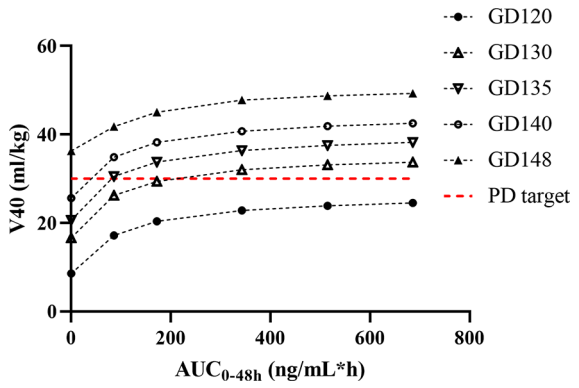

Figure 5. Simulated exposure (AUC_{0-48h}) and end point (V40) of fetal sheep during GD 120−148. The morphologic lung maturation stages of GD120,130, 135, 140, and 148 in fetal sheep were similar to those of 28, 32, 34, 36, and 40 GW in human fetus, respectively.[30] PD target set as the V40 value of fetal lung maturation of 30 L in humans.

optimal approach to enhance the effectiveness and safety of clinical DEX applications.

In the current model, we did not consider the placental metabolism of DEX, and simplified the maternal-fetal transfer process of Cort. DEX and Cort are primarily metabolized by the enzyme 11βHSD-2 in the placenta.[33] The amount of only 13% DEX was metabolized by 11βHSD-2, while Cort was extensively metabolized in the placenta. The main source of Cort in fetus was self-secretion during the early and middle pregnant stages.[33] At the late pregnant stage, the activity and amount of 11βHSD-2 was significantly decreased, while the amount of 11βHSD-1 was substantially increased.[17] This shift enables the conversion of Cort metabolized by 11βHSD-2, leading to a significant transfer of maternal Cort to the fetal side.[17,34] In this study, we used the observed data to establish a regression equation to describe the fetal Cort dynamic changes with gestational age (as shown in Figure 2A).[22] This dynamic change of fetal endogenous cortisone (Cort_bl) was taken into account in our PD model (eqs 5−7), which simplified the Cort trans-placenta process in the current model.

DEX promoting fetal lung maturation was primarily based on its binding to the glucocorticoid receptors (GR), forming a steroid-receptor complex (SR). This complex enters the cell nucleus to exert genomic effects and subsequently promotes the maturation of fetal type II alveolar cells to promote the fetal lung maturation.[17] Therefore, when we established the PD model, it is crucial to consider the dynamic changes of endogenous corticosterone (Cort), as well as the competitive binding of Cort and DEX to GR. If we directly modeled the inhibition effect of Cort secretion by DEX, the Cort swiftly returned to the baseline once the DEX concentration disappeared, which did not reflect the physiological situation. Therefore, this study referred to the corticosterone competition model established by Sriram et al.[35] In this model, it was assumed that DEX and Cort competitively bind to GR to format SR with different affinities. Additionally, after DEX administration, the secretion of endogenous Cort was continuously suppressed with the feedback influence of the hypothalamic-pituitary-adrenal axis. Hence, the current model could well describe the inhibition and feedback effect of DEX

https://doi.org/10.1021/acsptsci.3c00391
ACS Pharmacol. Transl. Sci. 2024, 7, 1770−1782

Table 4. Preclinical Pharmacokinetics and Pharmacodynamics Data Source of DEX in Different Animal Species[a]

aim	data	description	animal species	number	dosage of administration	administration route	gestational age (days)	sampling number	data Source
PK model development	DEX profile	DEX PK profiles of mother and fetus	pregnant sheep	8	12 mg single dose	i.m.	128−133	10	ref 22
	DEX profile	DEX PK profiles	nonpregnant monkey	6	0.04 mg/kg single dose 0.15 mg/kg single dose	oral		5	ref 18
	DEX profile	DEX PK profiles of mother and fetus	pregnant monkey	4	0.15 mg/kg Q24 h for 2 times	oral	130 ± 3	3	ref 18
PD-end point model development	Cort	physiological Cort development curve	pregnant sheep	5			110−145	NA	ref 41
	$Cort_{DEX}$	Cort curve under DEX administration	pregnant sheep	8	12 mg single dose	i.m.	128−133	10	ref 22
	GR	abundance of glucocorticoid receptors in fetal sheep lung	pregnant sheep	3			119−128		ref 42
	K_{D_DEX}	dissociation constant between DEX and GR	pregnant sheep	3			119−128		ref 42
	$DSPC_{trachea}$	daily tracheal outflow of DSPC	pregnant sheep	9	400 μg single dose	i.v. to the fetal jugular vein	113−147	25	ref 23
	$DSPC_{lung}$	lung concentration of DSPC	pregnant sheep	12			118−148	19	ref 27
	V40	lung volume of fetal sheep under trachea pressure of 40 cm H_2O	pregnant sheep	12			118−148	19	ref 27
model verification	V40	lung volume of fetal sheep under trachea pressure of 40 cm H_2O	pregnant sheep	9	0.25 mg/kg Q 24 h for 2 times	i.m.	122 ± 10	1	ref 20
	V40		pregnant sheep	22	6 mg Q 12 h for 4 times	i.m.	124.1 ± 0.6	1	ref 28
	V40		pregnant monkey	13	0.04 mg/kg Q 6 h for 4 times 0.15 mg/kg Q 12 h for 3 times	oral	130 ± 2	1	ref 18

[a]i.m.: intramuscular injection; oral: oral administration; i.v.: intravenous injection. NA: not available.

https://doi.org/10.1021/acsptsci.3c00391
ACS Pharmacol. Transl. Sci. 2024, 7, 1770−1782

on endogenous Cort, as well as the gradual recovery of Cort after the cessation of DEX treatment.

We developed the quantitative PK/PD/end point relationship in pregnant sheep and monkeys to inform the clinical effective exposure of DEX in pregnant women of different gestational stages. In the current model, we innovatively linked the maternal-fetal PK model to the efficacy marker (DSPC) and disease end point (V40) for quantitative analysis of DEX exposure-efficacy. We selected the AUC_{0-48} as the exposure metric based on the clinical dose regimen of DEX (Q12h for 4 times). In addition, after DEX administration, the GR level was significantly higher than the SR (DEX and GR complex) level. This observation suggested that the binding process between DEX and GR was far from saturation, with the SR complex dynamically changing during the DEX administration process (Figure S3). Hence, the cumulative exposure of AUC_{0-48} serves as a more suitable exposure metric linked to the DEX efficacy. DSPC is the primary active component in phosphatidylcholine. Phosphatidylcholine and surfactant proteins constitute the pulmonary surfactant, which was the material foundation for alveolar development.[36−38] DEX could increase the activity of phosphocholine cytidine transferase (PCT) by enhancing the production of DSPC through the cytidine diphosphate-choline pathway.[39] We selected the tracheal secretion DSPC (DSPC_trachea) as the primary PD marker for model development based on the following reasons: (1) DSPC in tracheal fluid has a good regression related with the fetal DSPC level and disease end point V40 (Figure 2E); (2) compared to other pulmonary surfactant proteins (SP-A/B/C/D, etc.), DSPC_trachea levels can be sampled multiple times during normal pregnancy, allowing continuous data for model development for monitoring of lung maturity in different gestational stages,[37,38] thus making it as a rational indicator for characterizing pulmonary surfactant quantity as well as the lung maturation progress.

Although this study preliminarily provided a useful strategy to indicate the DEX clinical exposure-response relationship of DEX, there still are some limitations in the current model. To simplify the model, regression equations were used to describe the relationship between DSPC in tracheal fluid and fetal lung as well as the relationship between DSPC lung concentration and V40. Consequently, these relationships are confined within a specific concentration range. In addition, for the pregnant monkey PK model, we failed to mechanistically adopt the perfusion-limited model to describe the passive diffusion part of trans-placental process of DEX. Despite attempting to fix the CLpd at the monkey placental blood flow rate of 3.09 L/h,[40] we encountered challenges due to insufficient data for model development, notably only 3 points for maternal PK and 3 points for fetal PK. Ultimately, we constructed a purpose-fitted PK model for pregnant monkeys, with the model parameters detailed in Table 1. All model simulations were conducted at the dose levels used during model development of 0.04 and 0.15 mg/kg, as illustrated in Figure 4A−C. Subsequently, the simulated fetal AUCs at 0.04 and 0.15 mg/kg were linked to the PD/end point model to simulate the fetal V40 at the same dose levels (Figure 5D). This pregnant monkey PK model effectively captured the fetal PK at current dose levels and further successfully validated the interspecies extrapolation of the PD-end point model in pregnant sheep. Additionally, as all the data were obtained from the published literature, only mean values were used for modeling, and therefore, this study could not predict the variability and confidence intervals. For E−R relationship interspecies extrapolation from pregnant sheep to pregnant monkeys, the V40 baseline was different between various species. However, after correction of the stages of morphologic lung maturation in different species, the V40 baseline was consistent between different species. Hence, we extrapolated the end point model interspecies by correcting the V40 baseline with the corresponding relationship between gestational phase and the stages of morphologic lung maturation in different species. Lastly, due to the scarcity of clinical DEX PK/PD/end point data in pregnant women, this study relied solely on simulations, emphasizing the need for further validation with clinical data.

3. CONCLUSIONS

In summary, this study provides an initial description of the relationship between DEX dosage, fetal exposure, and efficacy. We accomplished this goal by developing a PK/PD/end point model for DEX in pregnant sheep and monkeys, which demonstrated an acceptable level of accuracy and precision. We verified the interspecies extrapolation of the current model and then applied it to simulate the fetal exposure-DSPC-V40 relationship in human fetuses. The simulated result indicated that an increased DEX dosage might require before 32 GW to facilitate optimal fetal lung development. On the other hand, the dose might be reduced after 32 GW to prevent the development of long-term neurotoxicity. However, this heightened dosage may pose challenges in the clinic. Hence, after 32 GW, it becomes imperative to reduce the DEX dosage to mitigate the risk of long-term neurotoxicity. This study used the model-informed approach to provide some preliminary considerations for the clinical dexamethasone dose optimization.

4. METHODS

4.1. Data Sources. *4.1.1. Modeling Data.* For PK modeling data, we searched Pubmed using the keywords as "dexamethasone" and "pharmacokinetics" in pregnant sheep and monkeys. We selected the articles according to the following criteria: (1) antenatal administration of DEX for fetal lung maturation; (2) the animal model is a pregnant sheep or monkey; (3) simultaneous maternal-fetal PK data for both DEX and Cort that can construct complete concentration−time curves. Finally, one article for pregnant sheep and one article for a pregnant monkey was selected, and the experiment design is shown in Table 4.[22]

For the PD-end point modeling data, we searched Pubmed using the keywords containing "cortisol", "cortisol under DEX administration", "glucocorticoid receptors", "daily tracheal outflow of DSPC", "lung concentration of DSPC", and "V40" in pregnant sheep and monkeys. We selected articles with the following criteria: (1) antenatal administration of DEX for fetal lung maturation; (2) the animal model is a pregnant sheep or monkey; (3) contained above PD markers and disease end points. We further excluded articles without continuous end point data with gestational age. Finally, four articles for pregnant sheep were selected and the experiment design is shown in Table 4.[22,23,27,42] There are no articles that meet the criteria for pregnant monkeys.

Notably, model development needed continuous PD and end point data with gestational age to fit PD-end point dynamic profiles. Hence, we used the continuous PD-end point data for model development and used the articles

https://doi.org/10.1021/acsptsci.3c00391
ACS Pharmacol. Transl. Sci. 2024, 7, 1770−1782

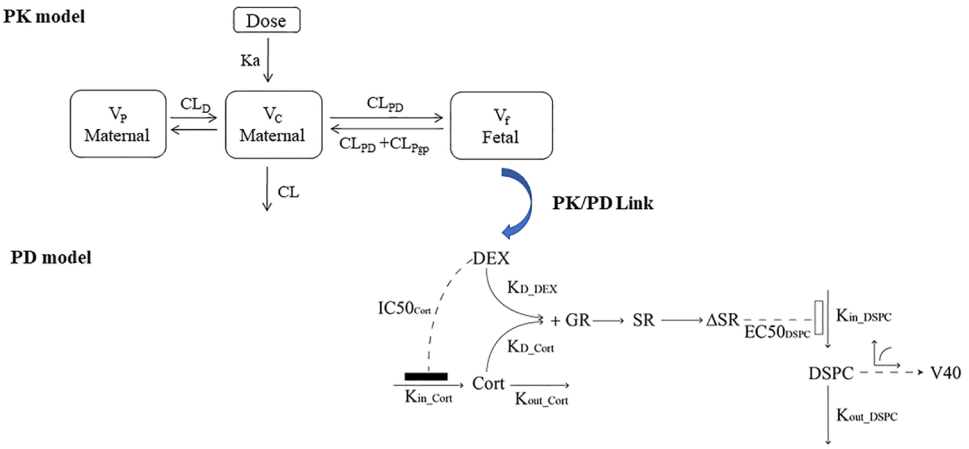

Figure 6. DEX PK/PD model of pregnant animals. PK model: maternal-fetal model structure. K_a represents the first-order elimination rate constant (the administration route for sheep and monkeys was intramuscular injection (i.m.) and oral administration); CL and V refer to clearance and volume of distribution; subscripts m, f, C, and P represent maternal, fetal, central, and peripheral compartment, respectively; CL_D represents the distribution clearance between the maternal central and peripheral compartment. CL_{PD} and CLp-gp represent the passive diffusion clearance rate and active efflux clearance of P-gp in the placenta transfer process. PD model: DEX effect mechanism diagram of fetal sheep. GR indicates the abundance of glucocorticoid receptors in the fetal lung; SR represents the concentration of DEX-GR complex in the fetal lung; $Cort_{DEX}$ refers to the concentration of Cort under DEX administration; K_{D_DEX} represents the dissociation constant between DEX and GR; K_{D_Cort} represents the dissociation constant between Cort and GR; K_{in} indicates the zero-order generation rate constant; K_{out} represents the first-order elimination rate; IC50 represents the half-maximum inhibitory concentration; and $Cort_{bl}$ represents the baseline level of Cort. The black rectangle means that DEX inhibited the endogenous cortisone; the white rectangle means that the ΔSR induced the DSPC.

containing single or discontinuous PD-end point data for model external verification.

4.1.2. External Verification Data for PD-End Point Model. For external verification data of the PD-end point in pregnant sheep and pregnant monkey, we conducted an extensive search on Pubmed using the same keywords listed in Section 4.1.1 of the PD-end point modeling data. Article selection criteria was also kept consistent as the above description in Section 4.1.1 only except for the following point: articles containing discontinuous data of PD or end point could be used for external verification. Finally, two articles were selected for pregnant sheep;[20,28] one article was included for pregnant monkeys. The experiment design is shown in Table 4.[18]

4.2. PK/PD/Disease Model Development in Pregnant Sheep. *4.2.1. PK Model.* The pregnant sheep PK model referred to the model structure described by Jusko et al.,[43] as shown in Figure 6. We adopted a three-compartment model to simultaneously simulate maternal and fetal PK characteristics in both pregnant sheep and monkeys. The maternal PK characteristics of DEX can be described by a two-compartment model, which has been validated in multiple species.[44] We assumed that DEX was only metabolized in maternal liver since the relative abundance of potential enzymes in placenta (11β -HSD, CYP3A4) and fetal liver (CYP3A4) were almost ignorable.[45] We described the placental transport process of DEX as two parts: passive diffusion clearance (CL_{PD}) and active efflux clearance of P-gp in placenta (CLp-gp). DEX was mainly transported by P-gp in placenta.[46] Due to the high permeability of DEX, we used a perfusion-limited model to describe the passive diffusion part of trans-placental process of DEX.[12] Therefore, the CL_{PD} of DEX was fixed as the placental blood flow in pregnant sheep.[24] The PK model equations were listed as below, where subscript IM refers to the intramuscular injection; $[A(0)]$ refers to the initial drug amount; K_a represents the first-order elimination rate constant; CL and V refer to the clearance and volume of distribution; F represents the bioavailability; subscripts m, f, C, and P represent the maternal, fetal, central, and peripheral compartment, respectively; CL_D represents the distribution clearance between the maternal central and peripheral compartment. The PK parameter description is listed in Table 2.

$$\frac{dA_{IM}}{dt} = -k_a \times A_{IM},\ A_{IM}(0) = \text{dose} \tag{1}$$

$$\frac{dA_{Cm}}{dt} = k_a \times A_{IM} - \left(\frac{CL/F}{V_C/F} + \frac{CL_D/F}{V_C/F} + \frac{CL_{PD}/F}{V_C/F}\right) \times A_C + \frac{CL_D/F}{V_P/F} \times A_P + \left(\frac{CL_{PD}/F}{V_f/F} + \frac{CL_{Pgp}/F}{V_f/F}\right) \times A_f,\ A_C(0) = 0 \tag{2}$$

$$\frac{dA_{Pm}}{dt} = \frac{CL_D/F}{V_C/F} \times A_C - \frac{CL_D/F}{V_P/F} \times A_P,\ A_P(0) = 0 \tag{3}$$

$$\frac{dA_{Cf}}{dt} = \frac{CL_{PD}/F}{V_C/F} \times A_C - \left(\frac{CL_{PD}/F}{V_f/F} + \frac{CL_{Pgp}/F}{V_f/F}\right) \times A_f,\ A_f(0) = 0 \tag{4}$$

4.2.2. PD-End Point Model. 4.2.2.1. Overall Model Structure of Mechanistic PD-End Point Model. The overall model structure of the mechanistic PD-end point model is shown in Figure 6. A large number of studies have shown that DEX mainly enters fetal alveolar type II cells, binds to the cytosolic GR, and forms a steroid−receptor complex (SR). Then, the complex enters the nucleus to promote the production of surface-active substances DSPC.[17] Finally, the surface-active substances drove the disease end point V40 of

https://doi.org/10.1021/acsptsci.3c00391
ACS Pharmacol. Transl. Sci. 2024, 7, 1770−1782

fetal lung maturation. Notably, it has been reported that DEX and Cort in the fetal chamber competitively combine GR to promote fetal lung maturation, and DEX can inhibit Cort secretion.[41]

4.2.2.2. Cort/DEX and GR Binding Model. The Cort/DEX and GR model structure is shown in Figure 6, which was referred to the published model structure.[19] DEX and Cort completely bound to GR in the cytoplasm with different affinities. The production process of SR was described as eq 5. The Cort profiles under the condition of DEX administration is described as eq 6. The negative feedback induced by DEX administration was described as an Emax effect on Kin of Cort.

The equation parameters are as follows: SR represents the concentration of DEX/Cort-GR complex in the fetal lung; GR indicates the abundance of glucocorticoid receptors in the fetal lung; $Cort_{DEX}$ refers to the concentration of Cort under DEX administration; K_{D_DEX} represents the dissociation constant between DEX and GR; K_{D_Cort} represents the dissociation constant between Cort and GR; K_{in} indicates the zero-order generation rate constant; K_{out} represents the first-order elimination rate; IC50 represents the half-maximum inhibitory concentration; $Cort_{bl}$ represents the baseline level of Cort; A_{cf} and V_{cf} represent the amount and distribution volume of fetal compartment, respectively. The initial value of SR (SR0) is shown in eq 8.

$$SR = \left(GR \times \frac{A_{Cf}/V_{Cf}}{K_{D\_DEX}} + GR \times \frac{Cort_{DEX}}{K_{D\_Cort}}\right) \Big/ \left(1 + \frac{A_{Cf}/V_{Cf}}{K_{D\_DEX}} + \frac{Cort_{DEX}}{K_{D\_Cort}}\right) \quad (5)$$

$$\frac{dCort_{DEX}}{dt} = K_{in_{Cort}} * \left(1 - \frac{A_{Cf}}{A_{Cf} + IC50_{Cort}}\right) - Cort_{DEX} \times K_{out_{Cort}},\ Cort_{DEX}(0) = Cort(0) \quad (6)$$

$$K_{in_{Cort}} = Cort_{bl} \times K_{out_{Cort}} \quad (7)$$

4.2.2.3. SR Complex-DSPC Model. Phospholipids and surfactant proteins constitute pulmonary surfactants and provide a material basis for alveolar formation. DSPC is an important pulmonary surfactant that directly related to lung maturation.[36−38] DEX can increase the activity of phosphocholine cytidine transferase (PCT) by enhancing the cytidine diphosphate choline pathway to promote DSPC production.[39]

In this study, we used complex SR to drive the PD marker DSPC profiles. To reduce the inconsistencies in SR levels caused by interindividual differences of physiological Cort concentration, we used ΔSR in the current model. An indirect response model (IDR) was employed to describe this process (shown in eqs 8−10). The DSPC concentration was modeled as in eq 11.

In the current model, SR0 represents the endogenous SR level produced by the physiological cortisol; K_{in_DSPC} represents the zero-order generation rate constant of DSPC; K_{out_DSPC} represents the first-order elimination rate of DSPC; DSPC indicates the daily DSPC amount discharge from the trachea; EC50 represents the half-maximum effective concentration, and E_{max} represents the maximum effective effect; $DSPC_{bl}$ represents the baseline level of DSPC; GR indicates the abundance of glucocorticoid receptors in the fetal lung.

$$SR0 = GR \times Cort_{bl}/(K_{D_{Cort}} + Cort_{bl}) \quad (8)$$

$$\Delta SR = SR - SR0,\ when \Delta SR < 0,\ \Delta SR = 0 \quad (9)$$

$$\frac{dDSPC}{dt} = K_{in_{DSPC}} \times \left(1 + E_{max} \times \frac{\Delta SR}{EC50_{DSPC} + \Delta SR}\right) - K_{out_{DSPC}} \times DSPC \quad (10)$$

$$K_{in_{DSPC}} = K_{out_{DSPC}} \times DSPC_{bl} \quad (11)$$

4.2.2.4. DSPC-Disease End point (V40) Model. Due to the strong correlation between DSPC tracheal effluents and DSPC lung concentration, the conversion equation between these two parameters was obtained using the regression equation. In addition, the study data showed that DSPC lung concentration was also highly correlated with end points V40 at different gestational ages, so we continued to use regression equations to fit DSPC lung concentration and V40.

4.2.2.5. External Verification of PD/Disease Model in Pregnant Sheep. The external PD data (including DSPC and V40) of pregnant sheep for model verification was obtained from the published literature as described in Section 4.1.2.

We simulated V40 at GD 124 using our current model. The administration regimen and sampling design were consistent with the trial design of the external verification study. Then, we compared the model-simulated data with the observed data to verify the current PD-disease model.

4.3. PK/PD/Disease Model Development in Pregnant Monkeys. *4.3.1. Model Development.* The PK/PD data of pregnant monkeys was obtained from published literature as described in Sections 4.1.1 and 4.1.2. However, only few PK data of pregnant monkeys was searched from published paper that could not support the maternal-fetal PK model development in pregnant monkeys. In addition, the administration route of DEX of pregnant monkeys (oral administration) in published data was different from that in pregnant sheep (intramuscular injection), making it difficult to directly use the PK model structure from pregnant sheep. Hence, we first developed the PK model in nonpregnant monkeys. Then, we fixed the parameters of nonpregnant monkeys to the maternal model compartment and added fetal compartment to develop the whole maternal-fetal PK model for pregnant monkeys. The model structure is shown in Figure.S4. The PD/disease model structure and parameters of pregnant monkeys kept consistent with that estimated from pregnant sheep, assuming that the PD-end point pathway in these two species was consistent due to the lacking GR and DSPC data in monkeys.

4.3.2. External Verification of PK/PD/Disease Model in Pregnant Monkeys. The external DEX exposure-V40 profiles of pregnant monkeys for model verification was obtained from published literature as described in Section 4.1.2. The fetal DEX exposure-V40 profiles were simulated in pregnant monkeys according to the trial design in published study of pregnant monkeys, and the model-simulated V40 level were compared with that in published data.

4.4. PK/PD/Disease Model Simulation and Extrapolation of Effective Human Exposure. Pregnant sheep are the classic animal to research the DEX therapeutic effect for fetal lung maturation. The current clinical dose regimen of DEX directly adopted the same dose regimen that was used in

https://doi.org/10.1021/acsptsci.3c00391
ACS Pharmacol. Transl. Sci. 2024, 7, 1770−1782

pregnant sheep.[6,7] In addition, our PD-end point model in pregnant sheep well verified the interspecies extrapolation in pregnant monkeys (results shown in Section 4.4). These cross-mapping results indicated that the SR-DSPC-V40 relationship of pregnant sheep could be well extrapolated to other species.

Hence, we extrapolated the fetal exposure-end point relationship of pregnant sheep to pregnant women. We first extrapolated the gestational phase from pregnant sheep to pregnant women based on the stages of morphologic lung maturation in these two species.[25] The stages of morphologic lung maturation of 28−34 GW of pregnant women was consistent with the GD120-GD148 of pregnant sheep.[25] The effective PD target of V40 was set as 30 mL/kg based on the following proofs: (i) the V40 of adult subject was 25 mL/kg, which was obtained via published pressure−volume curves acquired by the slow constant-flow method and supersyringe method showed (human body weight of 60 kg);[31] (ii) the proof that fetal V40 was slightly higher than that of adults.[25,47] Based on the assumption that the exposure-PD-end point relationship was consistent between pregnant sheep and pregnant women, the exposure of DEX that reached 30 mL/kg of V40 during GW28−34 of pregnant women was defined as the target efficacy exposure.

■ ASSOCIATED CONTENT

Supporting Information

The Supporting Information is available free of charge at https://pubs.acs.org/doi/10.1021/acsptsci.3c00391.

Model sensitivity analysis and steroid-receptor complex curve of pregnant sheep as well as the dexamethasone PK model structure of nonpregnant monkeys (PDF)

■ AUTHOR INFORMATION

Corresponding Authors

Yuan Wei − *Department of Obstetrics and Gynecology, Peking University Third Hospital, Beijing 100191, China*; Phone: 010-82267646; Email: weiyuanbysy@163.com

Yangyu Zhao − *Department of Obstetrics and Gynecology, Peking University Third Hospital, Beijing 100191, China*; Phone: 010-82267646; Email: zhaoyangyu001@163.com

Dongyang Liu − *Drug Clinical Trial Center, Peking University Third Hospital, Beijing 100191, China; Institute of Medical Innovation and Research, Peking University Third Hospital, Beijing 100191, China*; orcid.org/0000-0002-0608-8192; Phone: 010-82265509; Email: liudongyang@vip.sina.com

Authors

Ling Song − *Department of Obstetrics and Gynecology, Peking University Third Hospital, Beijing 100191, China; Drug Clinical Trial Center, Peking University Third Hospital, Beijing 100191, China*

Jie Song − *Drug Clinical Trial Center, Peking University Third Hospital, Beijing 100191, China*

Ying Wang − *Department of Obstetrics and Gynecology, Peking University Third Hospital, Beijing 100191, China*

Complete contact information is available at: https://pubs.acs.org/10.1021/acsptsci.3c00391

Author Contributions

#L.S., J.S., and Y.W. equally contributed to this study.

Author Contributions

D.L. and L.S. designed the study. L.S. and J.S. collected the PK/PD/end point data and performed the modeling and simulations for DEX. Y.W. was responsible for quality control of the current work. Y.W., Y.Z., and D.L. revised the manuscript critically for valuable intellectual content and proofreading. L.S. wrote and finalized the manuscript.

Notes

The authors declare no competing financial interest.

■ ACKNOWLEDGMENTS

The study was supported by the National Natural Science Foundation of China (no. 82173895; 82373954); National Key Research and Development Program of China (2023YFC2705900); and The Bill & Melinda Gates Foundation, grant/award number: INV-007625.

■ ABBREVIATIONS USED

$A(0)$, initial drug amount; A_{cf}, the amount of fetal compartment; AUC, area under the curve; C_{max}, drug concentration maximum; CL, clearance; CL_{PD}, passive diffusion clearance; CLp-gp, active efflux clearance of P-gp in placenta; Cort, cortisol; $Cort_{bl}$, the baseline level of Cort; DEX, dexamethasone; DSPC, disaturated-phosphatidylcholine; E_{max}, the maximum effective effect; EC50, the half-maximum effective concentration; F, bioavailability; GD, gestational days; GR, glucocorticoid receptor; GW, gestational weeks; K_{D_DEX}, the dissociation constant between DEX and GR; IC50, the half-maximum inhibitory concentration; IM, intramuscular injection; K_a, first-order elimination rate constant; K_{D_Cort}, the dissociation constant between Cort and GR; K_{in}, the zero-order generation rate constant; K_{out}, the first-order elimination rate; NRDS, neonatal respiratory distress syndrome; PD, pharmacodynamics; PK, pharmacokinetics; SR, steroid-receptor complex; V, volume of distribution; V40, lung volume of fetal sheep under trachea pressure of 40 cm H_2O; V_{cf}, the distribution volume of fetal compartment

■ REFERENCES

(1) Howson, C. P.; Kinney, M. V.; McDougall, L.; Lawn, J. E.; Born Too Soon Preterm Birth Action Group. Born too soon: preterm birth matters. *Reprod. Health* **2013**, *10* (Suppl 1), S1.

(2) Yadav, S.; Lee, B.; Kamity, R. *Neonatal Respiratory Distress Syndrome*. In StatPearls Publishing: Treasure Island (FL), 2023.

(3) Smith, P. B.; Ambalavanan, N.; Li, L.; Cotten, C. M.; Laughon, M.; Walsh, M. C.; Das, A.; Bell, E. F.; Carlo, W. A.; Stoll, B. J.; Shankaran, S.; Laptook, A. R.; Higgins, R. D.; Goldberg, R. N.; The Generic Database Subcommittee; Eunice Kennedy Shriver National Institute of Child Health; Human Development Neonatal Research Network. Approach to infants born at 22 to 24 weeks' gestation: relationship to outcomes of more-mature infants. *Pediatrics* **2012**, *129* (6), e1508−e1516.

(4) Yan, J. M.; Huang, H.; Li, Q. Q.; Deng, X. Y. A single-center study on the incidence and mortality of preterm infants from 2006 to 2016. *Zhongguo Dang Dai Er Ke Za Zhi* **2018**, *20* (5), 368−372.

(5) Opinion, C. Committee Opinion No. 713 Summary: Antenatal Corticosteroid Therapy for Fetal Maturation. *Obstet. Gynecol.* **2017**, *130* (2), 493−494.

(6) Liggins, G. C. Premature delivery of foetal lambs infused with glucocorticoids. *J. Endocrinol* **1969**, *45* (4), 515−23.

(7) Liggins, G. C.; Howie, R. N. A controlled trial of antepartum glucocorticoid treatment for prevention of the respiratory distress syndrome in premature infants. *Pediatrics* **1972**, *50* (4), 515−25.

(8) Wynne, K.; Rowe, C.; Delbridge, M.; Watkins, B.; Brown, K.; Addley, J.; Woods, A.; Murray, H. Antenatal corticosteroid

administration for foetal lung maturation. *F1000Research* **2020**, *9*, 219.
(9) Roberts, D.; Dalziel, S. Antenatal corticosteroids for accelerating fetal lung maturation for women at risk of preterm birth. *Cochrane database of systematic reviews* **2006**, No. 3, Cd004454.
(10) Ninan, K.; Liyanage, S. K.; Murphy, K. E.; Asztalos, E. V.; McDonald, S. D. Evaluation of Long-term Outcomes Associated With Preterm Exposure to Antenatal Corticosteroids: A Systematic Review and Meta-analysis. *JAMA Pediatr* **2022**, *176* (6), No. e220483.
(11) Anoshchenko, O.; Storelli, F.; Unadkat, J. D. Successful Prediction of Human Fetal Exposure to P-Glycoprotein Substrate Drugs Using the Proteomics-Informed Relative Expression Factor Approach and PBPK Modeling and Simulation. *Drug metabolism and disposition: the biological fate of chemicals* **2021**, *49* (10), 919−928.
(12) Anoshchenko, O.; Milad, M. A.; Unadkat, J. D. Estimating fetal exposure to the P-gp substrates, corticosteroids, by PBPK modeling to inform prevention of neonatal respiratory distress syndrome. *CPT Pharmacometrics Syst. Pharmacol* **2021**, *10* (9), 1057−1070.
(13) Krzyzanski, W.; Milad, M. A.; Jobe, A. H.; Jusko, W. J. Minimal physiologically-based hybrid model of pharmacokinetics in pregnant women: Application to antenatal corticosteroids. *CPT Pharmacometrics Syst. Pharmacol* **2023**, *12* (5), 668−680.
(14) Kream, J.; Mulay, S.; Fukushima, D. K.; Solomon, S. Determination of plasma dexamethasone in the mother and the newborn after administration of the hormone in a clinical trial. *J. Clin Endocrinol Metab* **1983**, *56* (1), 127−33.
(15) Leung-Pineda, V.; Gronowski, A. M. Biomarker tests for fetal lung maturity. *Biomark Med.* **2010**, *4* (6), 849−57.
(16) Chan, P.; Peskov, K.; Song, X. Applications of Model-Based Meta-Analysis in Drug Development. *Pharm. Res.* **2022**, *39* (8), 1761−1777.
(17) Busada, J. T.; Cidlowski, J. A. Mechanisms of Glucocorticoid Action During Development. *Curr. Top Dev Biol.* **2017**, *125*, 147−170.
(18) Schmidt, A. F.; Kemp, M. W.; Milad, M.; Miller, L. A.; Bridges, J. P.; Clarke, M. W.; Kannan, P. S.; Jobe, A. H. Oral dosing for antenatal corticosteroids in the Rhesus macaque. *PLoS One* **2019**, *14* (9), No. e0222817.
(19) Samtani, M. N.; Pyszczynski, N. A.; Dubois, D. C.; Almon, R. R.; Jusko, W. J. Modeling glucocorticoid-mediated fetal lung maturation: II. Temporal patterns of gene expression in fetal rat lung. *Journal of pharmacology and experimental therapeutics* **2006**, *317* (1), 127−38.
(20) Schmidt, A. F.; Kemp, M. W.; Kannan, P. S.; Kramer, B. W.; Newnham, J. P.; Kallapur, S. G.; Jobe, A. H. Antenatal dexamethasone vs. betamethasone dosing for lung maturation in fetal sheep. *Pediatric research* **2017**, *81* (3), 496−503.
(21) Schmidt, A. F.; Jobe, A. H.; Kannan, P. S.; Bridges, J. P.; Newnham, J. P.; Saito, M.; Usuda, H.; Kumagai, Y.; Fee, E. L.; Clarke, M.; Kemp, M. W. Oral antenatal corticosteroids evaluated in fetal sheep. *Pediatr. Res.* **2019**, *86* (5), 589−594.
(22) Bennet, L.; Kozuma, S.; McGarrigle, H. H.; Hanson, M. A. Temporal changes in fetal cardiovascular, behavioural, metabolic and endocrine responses to maternally administered dexamethasone in the late gestation fetal sheep. *British journal of obstetrics and gynaecology* **1999**, *106* (4), 331−9.
(23) Taeusch, H. W., Jr.; Brown, E.; Torday, J. S.; Nielsen, H. C. Magnitude and duration of lung response to dexamethasone in fetal sheep. *Am. J. Obstet. Gynecol.* **1981**, *140* (4), 452−455.
(24) Oddy, V. H.; Gooden, J. M.; Hough, G. M.; Teleni, E.; Annison, E. F. Partitioning of nutrients in merino ewes. II. Glucose utilization by skeletal muscle, the pregnant uterus and the lactating mammary gland in relation to whole body glucose utilization. *Aust. J. Biol. Sci.* **1985**, *38* (1), 95−108.
(25) Ballard, P. L., Hormones and Lung Maturation. In *Monographs on Endocrinology*, 1 ed.; Springer Berlin: Heidelberg: USA, 1986; p p6. Table 1.1.
(26) Higuchi, M.; Hirano, H.; Gotoh, K.; Takahashi, H.; Maki, M.; Murakami, N.; Ikenoue, T. Correlation between disaturated phosphatidylcholine in amniotic fluid and fetal lung maturation. *Nihon Sanka Fujinka Gakkai Zasshi* **1987**, *39* (10), 1715−1722.
(27) Warburton, D.; Parton, L.; Buckley, S.; Cosico, L.; Saluna, T. Effects of glucose infusion on surfactant and glycogen regulation in fetal lamb lung. *J. Appl. Physiol.* **1987**, *63* (5), 1750−1756.
(28) Usuda, H.; Fee, E. L.; Carter, S.; Furfaro, L.; Takahashi, T.; Takahashi, Y.; Newnham, J. P.; Milad, M. A.; Saito, M.; Jobe, A. H.; Kemp, M. W. Low-dose antenatal betamethasone treatment achieves preterm lung maturation equivalent to that of the World Health Organization dexamethasone regimen but with reduced endocrine disruption in a sheep model of pregnancy. *Am. J. Obstet. Gynecol.* **2022**, *227* (6), 903.e1−903.e16.
(29) Usuda, H.; Fee, E. L.; Carter, S.; Furfaro, L.; Takahashi, T.; Takahashi, Y.; Newnham, J. P.; Milad, M. A.; Saito, M.; Jobe, A. H.; Kemp, M. W. Low-dose antenatal betamethasone treatment achieves preterm lung maturation equivalent to that of the World Health Organization dexamethasone regimen but with reduced endocrine disruption in a sheep model of pregnancy. *Am. J. Obstet. Gynecol.* **2022**, *227* (6), 903.e1−903.e16.
(30) Alcorn, D. G.; Adamson, T. M.; Maloney, J. E.; Robinson, P. M. A morphologic and morphometric analysis of fetal lung development in the sheep. *Anat Rec* **1981**, *201* (4), 655−67.
(31) Harris, R. S. Pressure-volume curves of the respiratory system. *Respir. Care* **2005**, *50* (1), 78−98.
(32) Schmitz, T.; Doret-Dion, M.; Sentilhes, L.; Parant, O.; Claris, O.; Renesme, L.; Abbal, J.; Girault, A.; Torchin, H.; Houllier, M.; Le Saché, N.; Vivanti, A. J.; De Luca, D.; Winer, N.; Flamant, C.; Thuillier, C.; Boileau, P.; Blanc, J.; Brevaut, V.; Bouet, P. E.; Gascoin, G.; Beucher, G.; Datin-Dorriere, V.; Bounan, S.; Bolot, P.; Poncelet, C.; Alberti, C.; Ursino, M.; Aupiais, C.; Baud, O. Neonatal outcomes for women at risk of preterm delivery given half dose versus full dose of antenatal betamethasone: a randomised, multicentre, double-blind, placebo-controlled, non-inferiority trial. *Lancet* **2022**, *400* (10352), 592−604.
(33) Seckl, J. R. Glucocorticoids, feto-placental 11 beta-hydroxysteroid dehydrogenase type 2, and the early life origins of adult disease. *Steroids* **1997**, *62* (1), 89−94.
(34) Hennessy, D. P.; Coghlan, J. P.; Hardy, K. J.; Scoggins, B. A.; Wintour, E. M. The origin of cortisol in the blood of fetal sheep. *J. Endocrinol* **1982**, *95* (1), 71−9.
(35) Sriram, K.; Rodriguez-Fernandez, M.; Doyle, F. J., 3rd Modeling cortisol dynamics in the neuro-endocrine axis distinguishes normal, depression, and post-traumatic stress disorder (PTSD) in humans. *PLoS Comput. Biol.* **2012**, *8* (2), No. e1002379.
(36) Bourbon, J. R.; Farrell, P. M. Fetal lung development in the diabetic pregnancy. *Pediatric research* **1985**, *19* (3), 253−67.
(37) Tsai, M. Y.; Shultz, E. K.; Williams, P. P.; Bendel, R.; Butler, J.; Farb, H.; Wager, G.; Knox, E. G.; Julian, T.; Thompson, T. R. Assay of disaturated phosphatidylcholine in amniotic fluid as a test of fetal lung maturity: experience with 2000 analyses. *Clinical chemistry* **1987**, *33* (9), 1648−51.
(38) Higuchi, M.; Hirano, H.; Gotoh, K.; Otomo, K.; Maki, M. Comparison of amniotic fluid disaturated phosphatidylcholine, phosphatidylglycerol and lecithin/sphingomyelin ratio in predicting the risk of developing neonatal respiratory distress syndrome. *Gynecologic and obstetric investigation* **1990**, *29* (2), 92−6.
(39) Spragg, R. G.; Li, J. Effect of phosphocholine cytidylyltransferase overexpression on phosphatidylcholine synthesis in alveolar type II cells and related cell lines. *Am. J. Respir. Cell Mol. Biol.* **2000**, *22* (1), 116−24.
(40) Lees, M. H.; Hill, J. D.; Ochsner, A. J., 3rd; Thomas, C. L.; Novy, M. J. Maternal placental and myometrial blood flow of the rhesus monkey during uterine contractions. *Am. J. Obstet Gynecol* **1971**, *110* (1), 68−81.
(41) Ballard, P. L.; Kitterman, J. A.; Bland, R. D.; Clyman, R. I.; Gluckman, P. D.; Platzker, A. C.; Kaplan, S. L.; Grumbach, M. M. Ontogeny and regulation of corticosteroid binding globulin capacity in plasma of fetal and newborn lambs. *Endocrinology* **1982**, *110* (2), 359−66.

https://doi.org/10.1021/acsptsci.3c00391
ACS Pharmacol. Transl. Sci. 2024, 7, 1770−1782

(42) Flint, A. P.; Burton, R. D. Properties and ontogeny of the glucocorticoid receptor in the placenta and fetal lung of the sheep. *Journal of endocrinology* **1984**, *103* (1), 31−42.
(43) Samtani, M. N.; Schwab, M.; Nathanielsz, P. W.; Jusko, W. J. Area/moment and compartmental modeling of pharmacokinetics during pregnancy: applications to maternal/fetal exposures to corticosteroids in sheep and rats. *Pharm. Res.* **2004**, *21* (12), 2279−92.
(44) Song, D.; Jusko, W. J. Across-species meta-analysis of dexamethasone pharmacokinetics utilizing allometric and scaling modeling approaches. *Biopharm Drug Dispos* **2021**, *42* (5), 191−203.
(45) Murphy, V. E.; Fittock, R. J.; Zarzycki, P. K.; Delahunty, M. M.; Smith, R.; Clifton, V. L. Metabolism of synthetic steroids by the human placenta. *Placenta* **2007**, *28* (1), 39−46.
(46) Mark, P. J.; Waddell, B. J. P-glycoprotein restricts access of cortisol and dexamethasone to the glucocorticoid receptor in placental BeWo cells. *Endocrinology* **2006**, *147* (11), 5147−52.
(47) Brumley, G. W.; Chernick, V.; Hodson, W. A.; Normand, C.; Fenner, A.; Avery, M. E. Correlations of mechanical stability, morphology, pulmonary surfactant, and phospholipid content in the developing lamb lung. *J. Clin. Invest.* **1967**, *46* (5), 863−73.

https://doi.org/10.1021/acsptsci.3c00391
ACS Pharmacol. Transl. Sci. 2024, 7, 1770−1782